CFD Analysis of Vertical Axis Wind Turbines in close proximity

Via email from M. Paraschivoiu October 2010

Marius Paraschivoiu[a], Chad X. Zhang [a], Selvanayagam Jeyatharsan[a], Norbert V. Dy[b], Farooq Saeed[c], Robert N. Thomas[d], Ion Paraschivoiu[b]

[a]Department of Mechanical and Industrial Engineering, Concordia University, Montreal, Quebec, CANADA

[b]Department of Mechanical Engineering, Ecole Polytechnique Montreal, Montreal, Quebec, CANADA

[c]Aerospace Engineering Department, King Fahd University of Petroleum and Minerals, Dhahran, Saudi Arabia

[d]Wind Harvest International

Abstract

This paper presents an analysis based on computational fluid dynamics of vertical axis wind turbines when placed in close proximity in a linear array. It has been noticed that VAWTs placed close to each other with counter rotation motions have a higher coefficient of power than a single turbine. This was termed the "coupled vortex effect". Two mechanisms have been identified to cause this increase in efficiency: the streamtube contraction effect and the vortex effect. The first is due to the blockage effect from neighboring turbines while the later is related to the neighboring turbine acting as a vortex that induces an increased flow field. This paper analyzes each of these effects and studies the influence of the turbine size and the rotation speed. The change of torque on each blade due to these effects is investigated for two different sizes of wind turbines.

1. Introduction

The placement of wind turbines is a critical parameter when harvesting wind energy. It is important not only because the wind power scales with wind velocity cubed but also because the wind turbines have to be located on a physical site either on land or offshore. Furthermore, wind turbines are placed together in what is called "a wind turbine farm". Wind turbine farm location is selected based on wind availability, appropriate land permit use and access to electrical power lines. Once a certain area is allocated the number of wind turbines to be places is finite. In fact due to clearance distance for Horizontal wind

turbines the number of these turbines is limited to a density of 10 ha/MW [1,2,3]. This clearing distance depends on the complex unsteady aerodynamics of the wake behind a turbine and these wakes need to be studied to optimize placement of HAWT [4,5,6]. Recently it has been observed that Vertical Wind turbines can be placed much closer together therefore maximizing the use of a specific location [7]. Furthermore, it can be conceived that a combination of HAWT and VAWT can be optimally placed in a given area. **This is a point key to Google that should be highlighted in the letter to Google.**

Different wind characteristics can be better used by either VAWT or HAWT. As a general rule, HAWT perform better for a uniform wind but tend to lose efficiency if the wind direction fluctuates frequently or for an upward sweep angle [8]. Contrarily VAWT are less affected by what is termed "dirty winds". Obviously, VAWT can perform for any direction of the wind but also if the direction fluctuates rapidly or if the wind is less uniform [9]. Therefore, VAWTs are good candidates when placed close to the ground or in an urban environment [8]. It was also discovered by Wind Harvest International (WHI) that an array of turbines placed in close proximity increase the coefficient of power [7]. This effect was termed the "coupled vortex effect" because a neighboring turbine acts as a vortex generating more wind. In a simple way a VAWT can be seen by a neighboring turbine as a point vortex and a dipole [10]. The point vortex accounts for the flow rotation and the dipole accounts for the flow blockage, both can lead to a higher effective wind velocity. In this paper, this effect is studied and quantified using Computational Fluid Dynamics (CFD).

CFD solves partial differential equations to simulate the flow. It ranges from Reynolds Average Navies Stokes (RANS) models to more advanced and computationally very demanding Large Eddy Simulations (LES) models. For wind turbines, CFD can be used to perform aerodynamic analysis [11]. This tool has significantly evolved and is routinely used in different industries to analyze and to design fluid systems. For wind energy, CFD still lacks the ability to capture all the flow features such as boundary layer separation and transition. Nevertheless CFD have the ability to predict quite accurately global features such as the power coefficient as seen in this paper.

The rest of this paper is as follows. The CFD model is presented next. This model is calibrated with experimental data in section 2: A CFD model for VAWT. The simulation of an array of wind turbines is presented and compared with experimental data in Section 3. Section 4 describes and analysis the mechanisms that increase the coefficient of power.

2. A CFD model for VAWT

The basics of the CFD model developed are presented in this section. The solution is very sensitive to three main parameters which are: the mesh, the values of y+ and the time step.

2.1 Geometry and mesh

Unsteady flow simulations are performed for a 2D section of a vertical axis wind turbine therefore the three dimensional effects are not accounted for. A typical geometry is shown in figure 1. The simulations are based on unsteady Reynolds Average Navier-Stokes equations coupled with the Spalard-Allmaras turbulence model available in the commercial CFD Code Fluent. It is assumed that the flow is fully turbulent. The computational domain includes two zones: a fixed zone for the far-field flow and a rotating zone that rotates with the blades. A sliding mesh technique is used between the two zones. The radius of the rotating zone is 1.053 R, where R is the radius of the rotor. Blades rotate around the central axis with angular velocity ω. A fixed velocity value is imposed at the inflow boundary and an outflow boundary is imposed downstream. For faster convergence the sides of the computational domain have symmetry boundary conditions. A parametric study was done to calculate the smallest distance between the sides and the rotor so that it does not influence the flow.

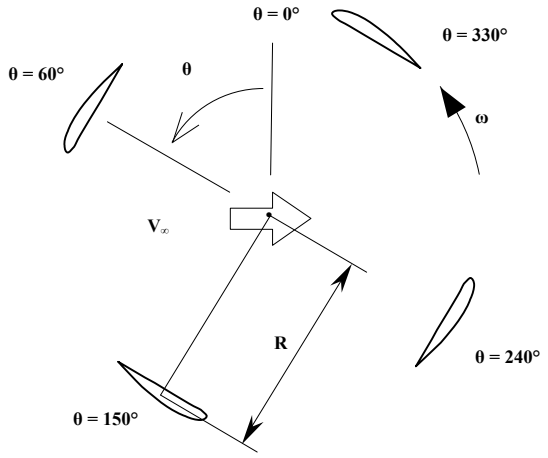

Figure 1: Typical four blade geometry.

A typical mesh around one wind turbine blade is illustrated in Figure 2a. A portion of the mesh which lies between the two rotors in an array of turbines in illustrated in Figure 2b. As seen the mesh is formed in blocks and is finer around the airfoil. The mesh outside the rotating region is much coarser. The flow simulation parameters used in Fluent are reported in Table 1.

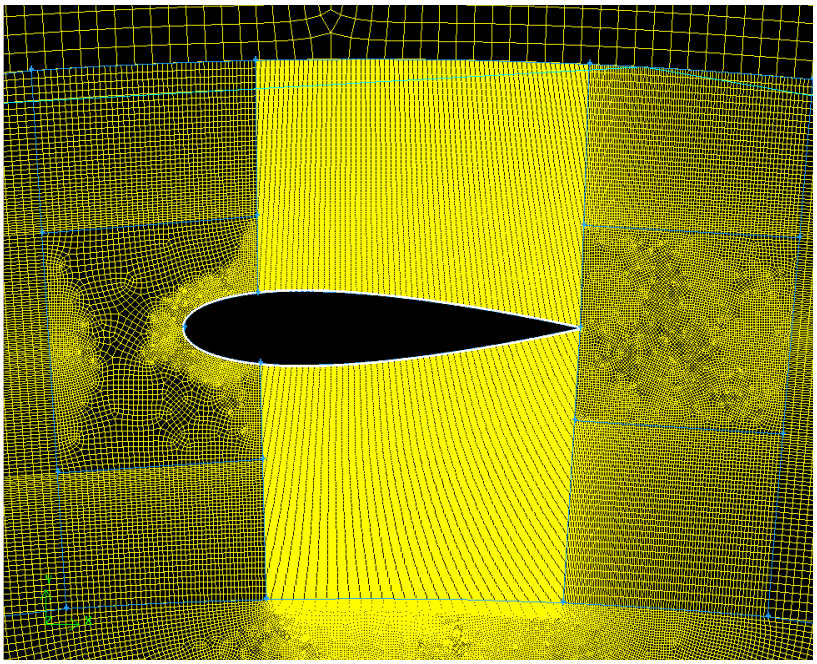

Figure 2a: Typical mesh around the wind turbine blade.

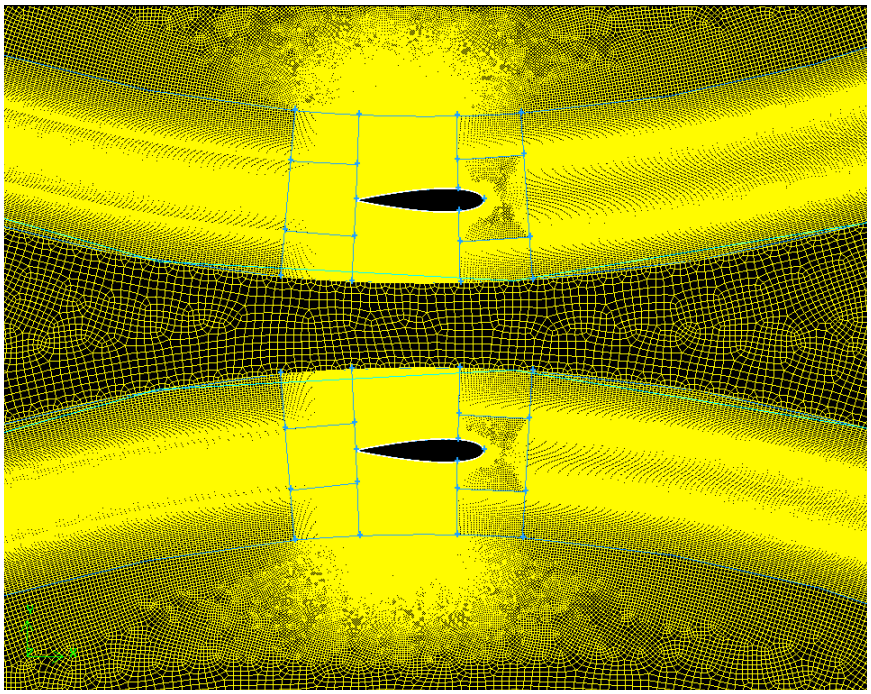

Figure 2b: Typical mesh used for an array of turbines.

CFD Data	
Version	Double precision
Viscous model	Spalart-Allmaras (1 egn)
Solver	Unsteady 2nd order implicit

Number of elements	1,193,618	
Number of nodes	1,198,546	
Convergence criteria	Continuity	$1e^{-8}$
	x-velocity	$1e^{-6}$
	Y velocity	$1e^{-6}$
	Nut	$1e^{-6}$
Time step size	0.003	
Number of processors used to run the job	8	

Table 1: Flow simulation parameters

2.2 Calibration and Validation of CFD model with data from WHI 530G:

The simulation model is calibrated for the WHI 530G turbine rotating at a fixed angular velocity of 90 rpm. The calibration is performed by changing the mesh and the time step until results do not change significantly.

To calculate the coefficient of power (CP) for different tip speed ratios (TSR), the wind speed is changed and a new CFD run is performed. Figure 3 shows the CP as a function of time for TSR =2. Note that initially the CP has a transient behavior before reaching a periodic oscillation. The coefficient of power is calculated for each blade and summed up for each instantaneous time.

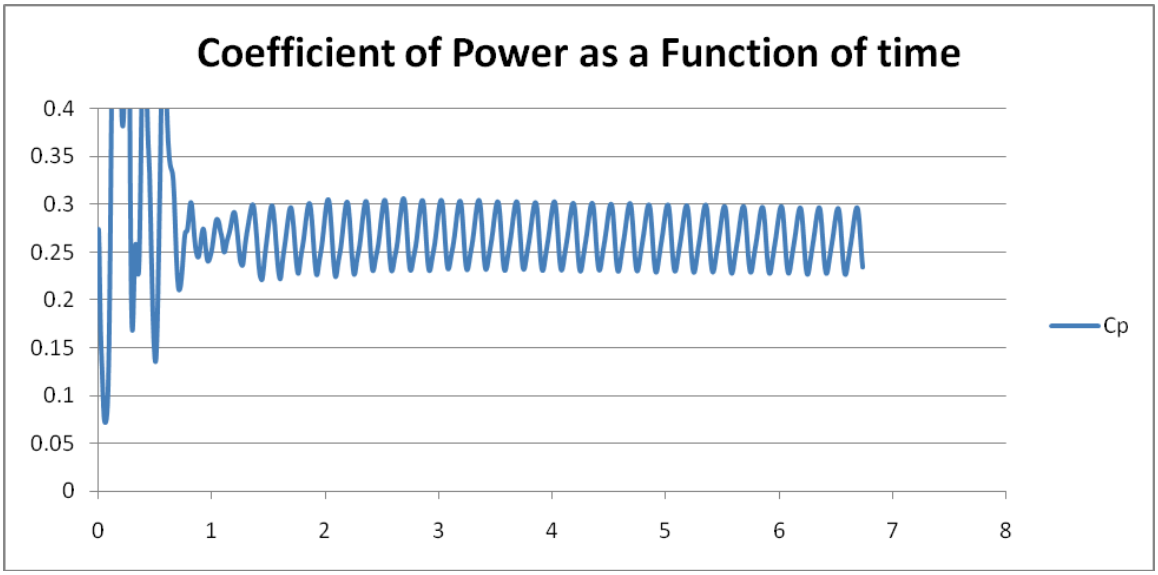

Figure 3: CP as a function of time (s) for one rotor at TSR = 2

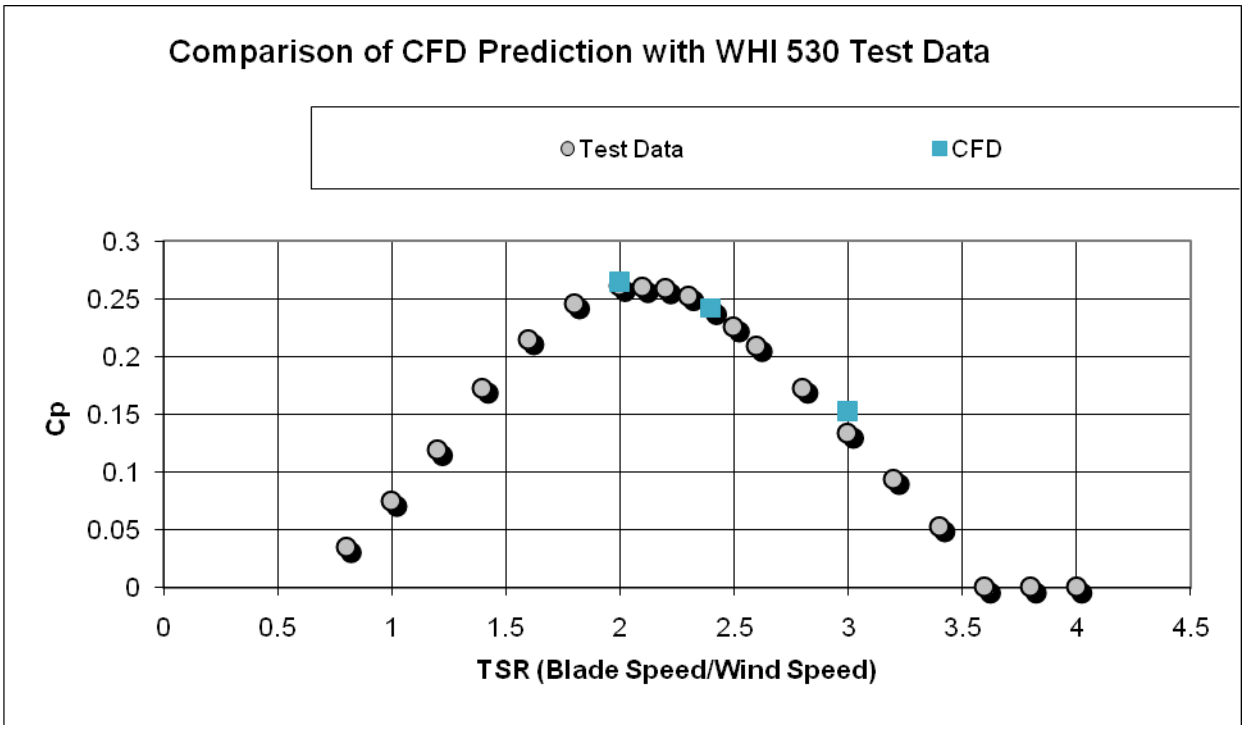

Figure 4: CFD data comparision with the test data.

In Figure 4 we compare three different CFD runs with the experimental data provided by WHI. In 2001, performance data was collected for a signle turbine located at Palm Spring. The daily electrical output and average wind speed were recorded and used in the calculation of the coefficent of power. The electric output was concerved into the shaft output by using an estimated power train efficency of 0.92 and an estimated gearbox efficency of 0.9325. The values of the three CFD runs are also reported in table 2 an show that the agreement is very good in particular for high CP values.

	CFD	*Test data*
1 rotor TSR = 2.0	0.265	0.261
1 rotor TSR = 2.4	0.242	0.241
1 rotor TSR = 3.0	0.153	0.134

Table 2: CFD and experimental comparison of the coefficient of power

Figure 5 and 6 show the time average values of the x component of velocity for the case of TSR 2. The color label, on the right, gives the values of velocity. Note that the average inside the circle (moving part of the domain) is not relevant as the domain rotates. The flow is from left to right and the turbine turns anti-clockwise. From both figures we note that the flow is slower in the first quadrant (blade travelling from the top to the middle) than on the second quadrant (blade traveling from the middle to the bottom). This indicates that the vortex generated by the turbine is influencing the flow field so that it is not symmetrical.

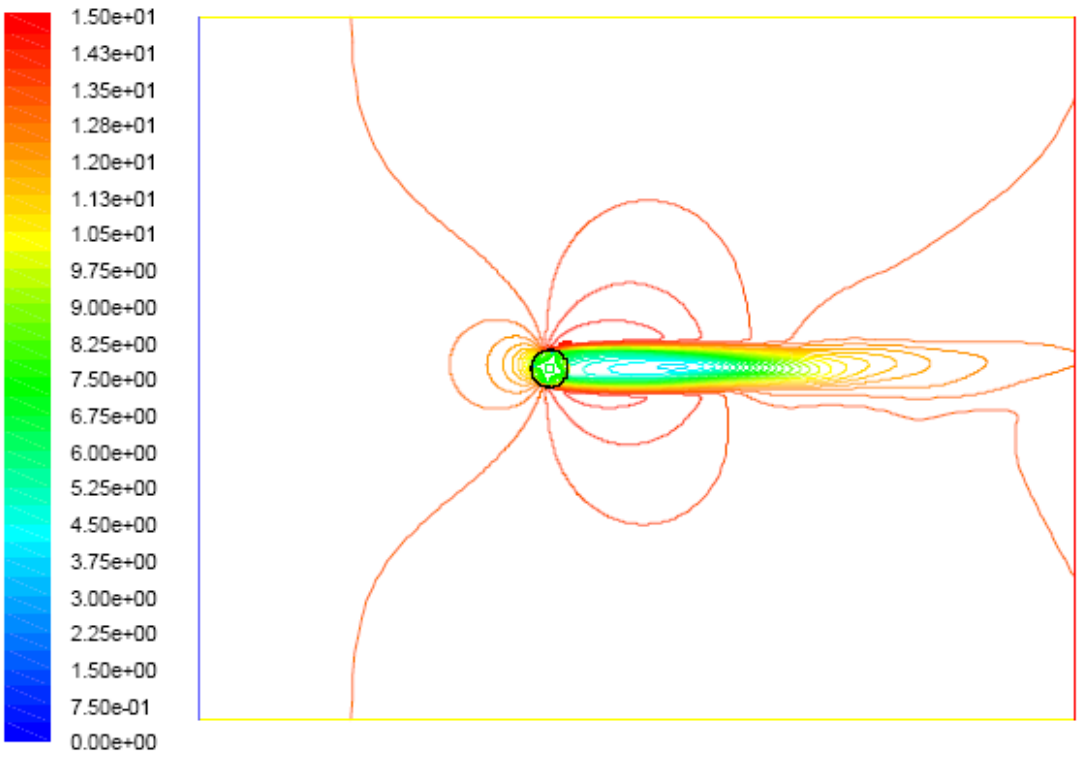

Figure 4: Average X velocity for one WHI 530G rotor

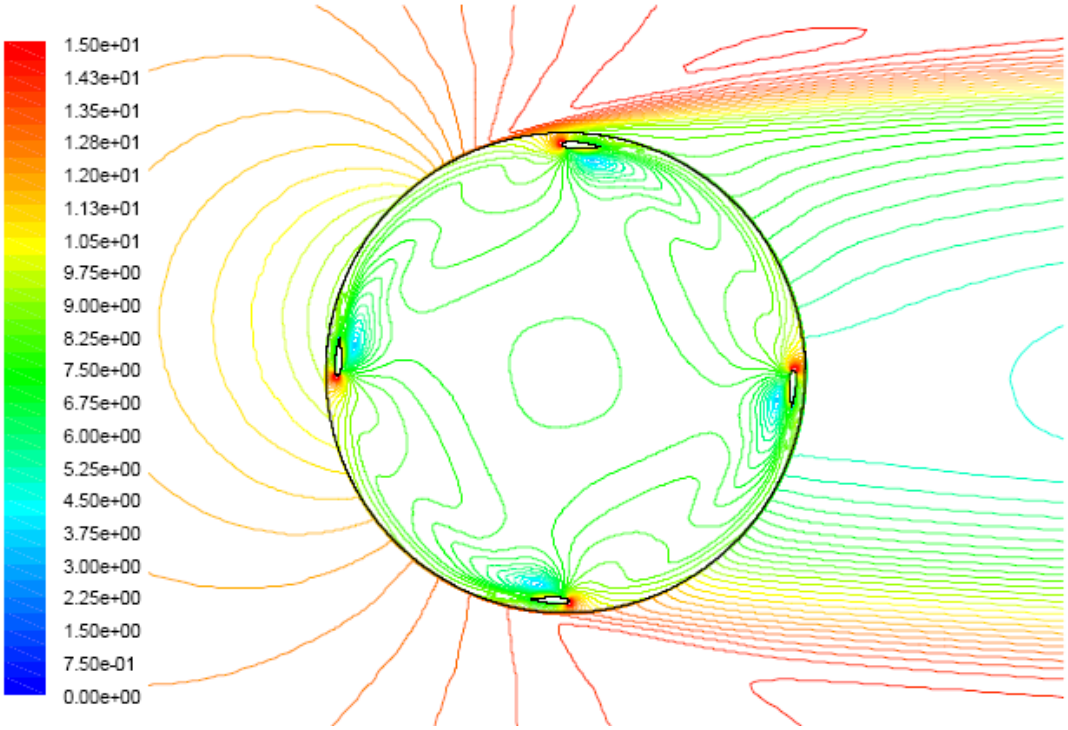

Figure 6: Close up of the average X velocity for one WHI 530G rotor

Simulation of a single WHI 3000:

CFD runs are now performed to simulate the flow around a 2D section of the WHI 3000 which is a larger diameter VAWT and therefore a lower solidity. The geometry and the flow simulation parameters for TSR = 2 are reported in Table 3. The same CFD model as described previously is used.

Number of blades	4
Blade chord	0.9753 m
Rotor Diameter (R)	23.88 m
RPM	29
Tip speed ratio (TSR)	2
Blade type	NACA0018
CFD Data	
Number of elements	1,193,618
Number of nodes	1,198,546
Moving mesh (rad /s)	3.036873
Free stream velocity (m/s)	18.1301
Density	1.1774
Dynamic viscosity	1.8462×10^{-5}

Table 3: Geometry and Flow simulation parameters

The power coefficient as a function of time is reported in Figure 7 for calculations at 5 different TSR values. The figure shows that after a transient period the CP oscillates around an average value. The oscillations are due to the unsteady flow behavior of the turbines. The time step used for these simulations is 0.003. To verify the time step chosen we have performed calculations at smaller time steps and obtained the same results. Time steps larger than 0.003 did not give correct values of CP.

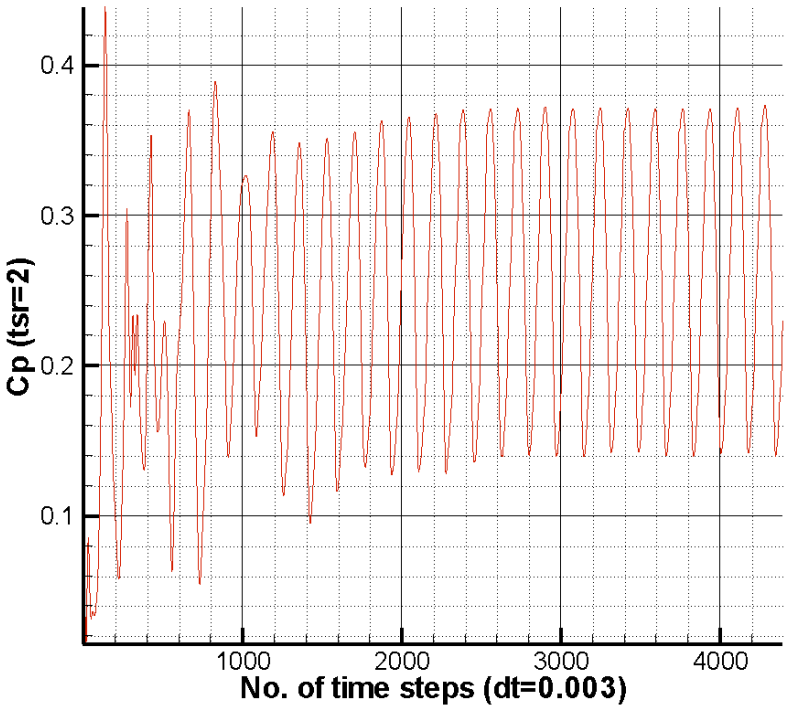

Figure 7a: Power coefficient as a function of number of iterations at TSR 2.

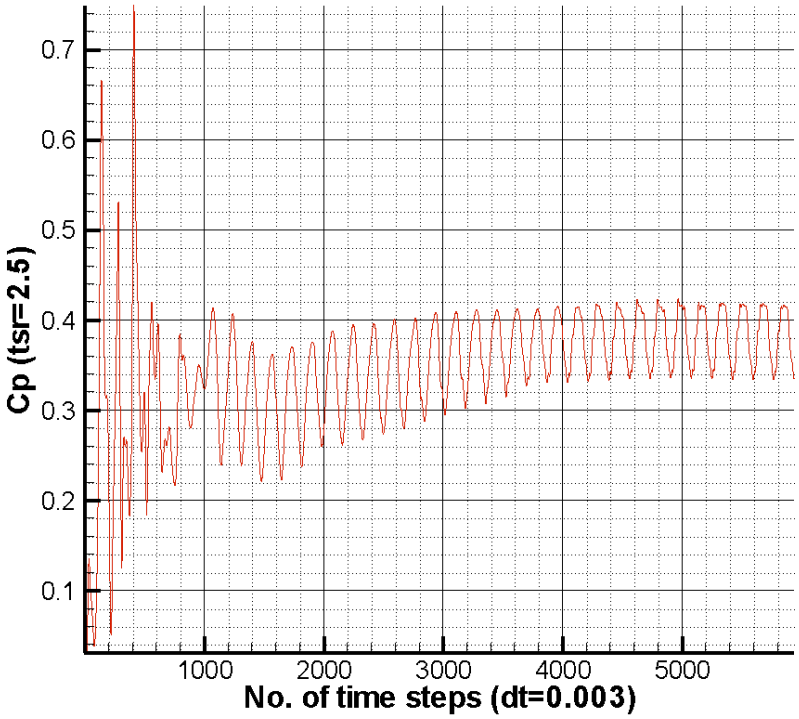

Figure 7b: Power coefficient as a function of number of iterations at TSR 2.5.

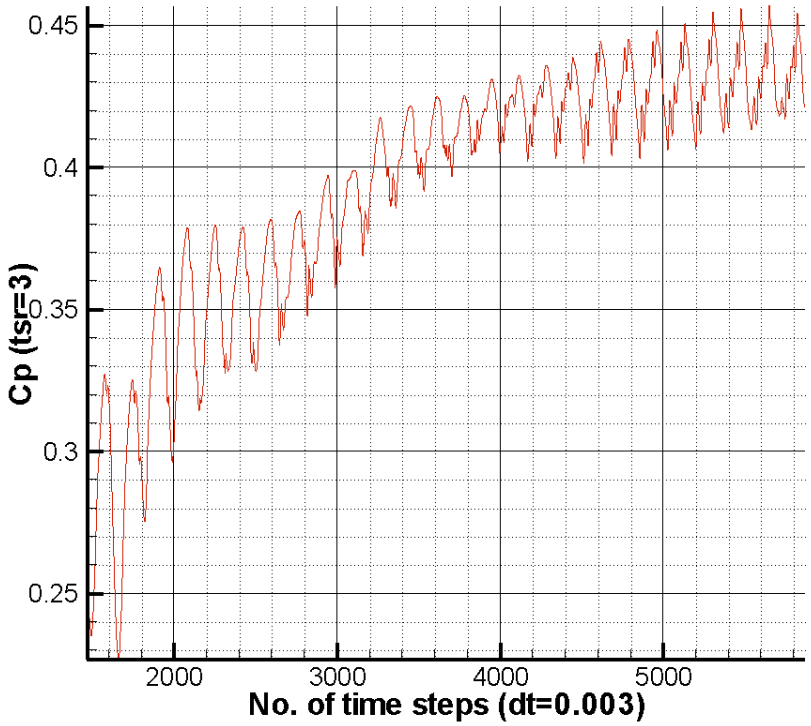

Figure 7c: Power coefficient as a function of number of iterations at TSR 3.

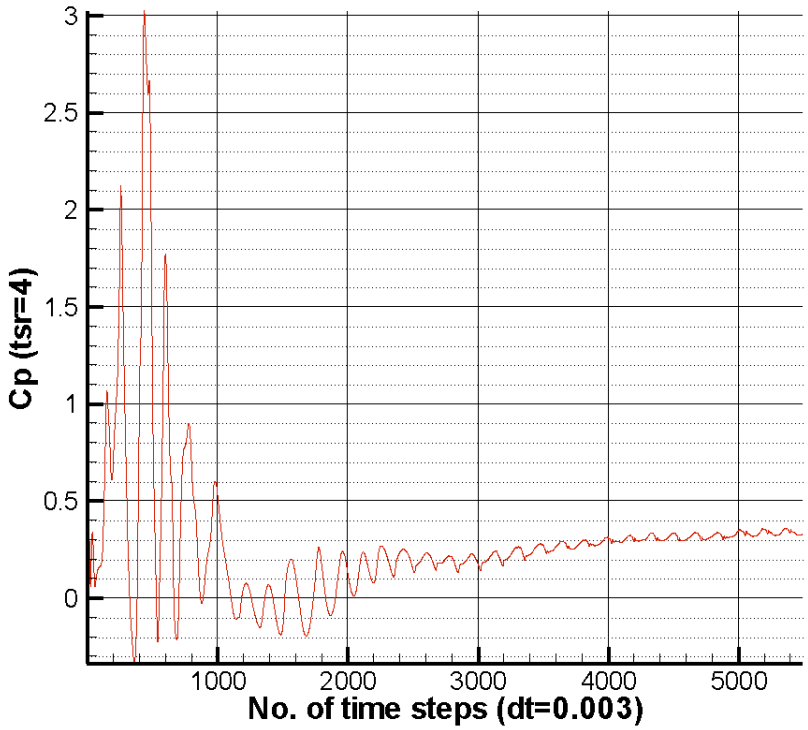

Figure 7d: Power coefficient as a function of number of iterations at TSR 4.

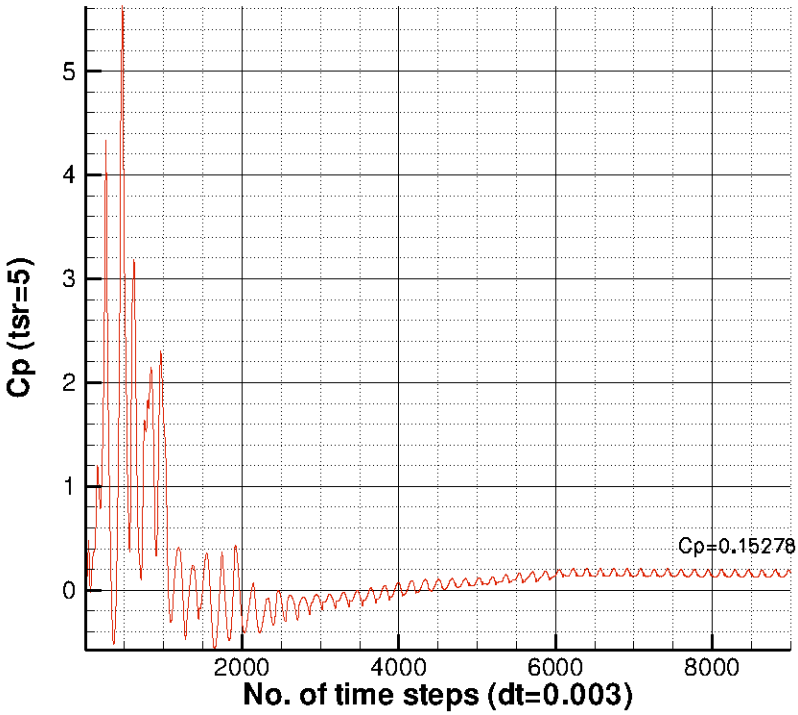

Figure 7e: Power coefficient as a function of number of iterations at TSR 5.

Figure 8 shows the iso-contours of the Average x component of velocity. The free stream velocity is 18.1 m/s. The rotating zone is bounded by the white circle. Note again that the flow is not symmetrical. The iso-contours on the bottom part are of higher value because the vortex speed is added while on the top the vortex speed is subtracted from the mean flow. We also see the blockage effect as the flow appears to go around the turbine.

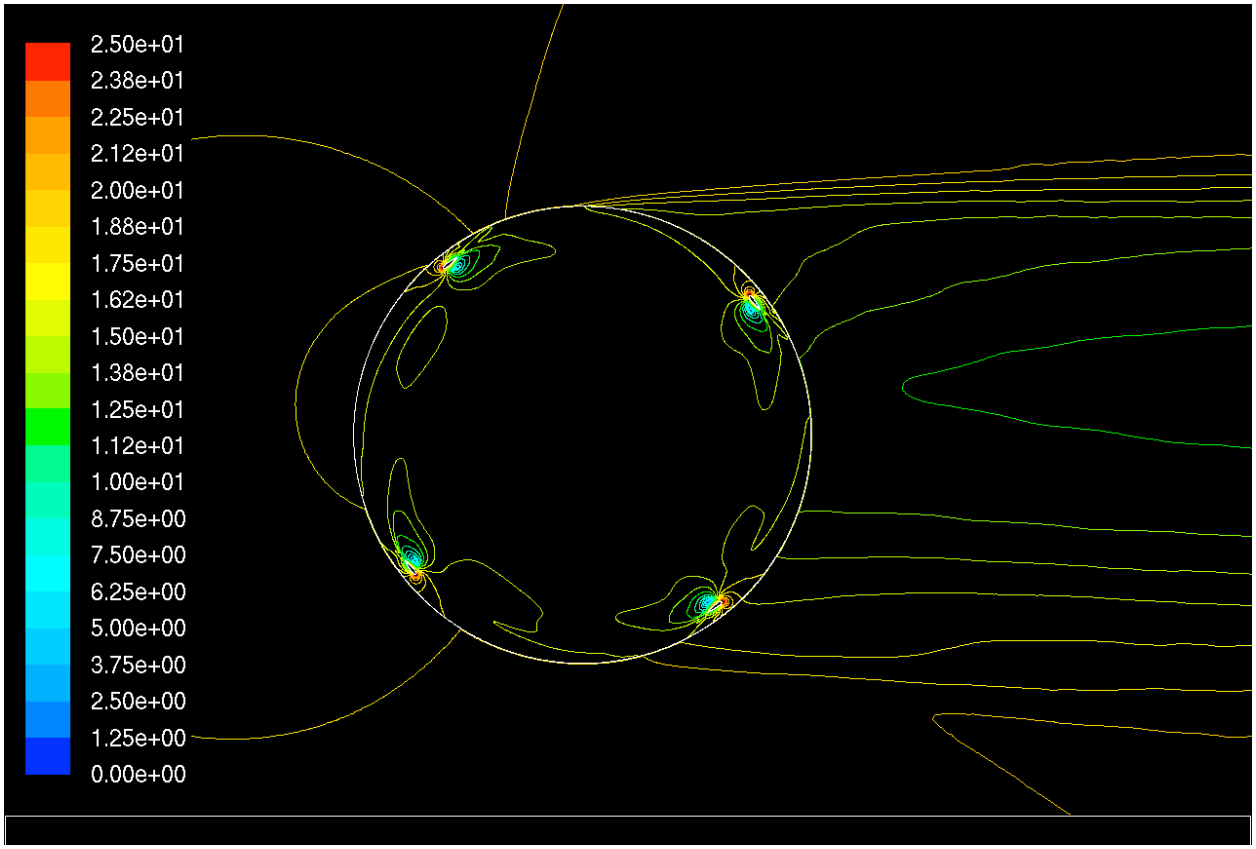

Figure 8: Average x component of velocity at TSR = 2

In Table 4 the power coefficent is reported and compared with CARDAAV [8] as experimental data is not available. Each calculation for one TSR takes approximately 4 days on an eight processor computer.

	CFD	*CARDAAV*
1 rotor TSR = 2.0	0.26	0.24
1 rotor TSR = 2.5	0.38	0.37
1 rotor TSR = 3.0	0.43	0.41
1 rotor TSR = 4.0	0.33	0.34
1 rotor TSR = 5.0	0.153	0.138

Table 4. Power coefficient comparison between CFD and CARDAAV for one rotor WHI 3000.

The CFD calculations are slightly above the CARDAAV values. This is expectable as the CFD is not modeling the struts and the center axis.

1. Simulation of an Array of three VAWTs

Two types of wind turbines are placed in a linear array facing the wind. First, the WHI 530G turbines are analyzed. These turbines rotate at 90 RPM. Second, the WHI 3000 turbines are investigated. These turbines rotate at a much lower rotation speed: 26 RPM.

3.1 Study of three WHI 530G placed in close proximity:

CFD is now used to simulate the flow over three WHI 530G type rotors placed in a linear array. The top rotor is rotating counter clockwise, the middle rotor is rotating clockwise and the bottom rotor is rotating counter clockwise. This simulation assumes a two dimensional flow as in the case of one rotor, so the flow from left to right at a constant height is simulated. The objective of this simulation is to study the effect of the proximity of two adjacent turbines placed on both sides of a turbine as seen in figure 9. The distance between the rotors axis is 1.08 rotor diameters.

A simulation run at TSR =2 (wind speed velocity of 12.65 m/s) is performed. The power coefficient (CP) calculated for the middle rotor is 0.331 while experimentally it was found to be 0.331.

	CFD	*Test data*
3 rotors TSR = 2.0	0.331	0.331

Figure 9 and 10 show the time average values of the x component of velocity. These iso-contours show a significant acceleration of the flow between the rotors. The iso-contours also show that when the blade is travelling towards the wind the effective wind velocity is reduced while when it is traveling away from the wind the effective flow is increased.

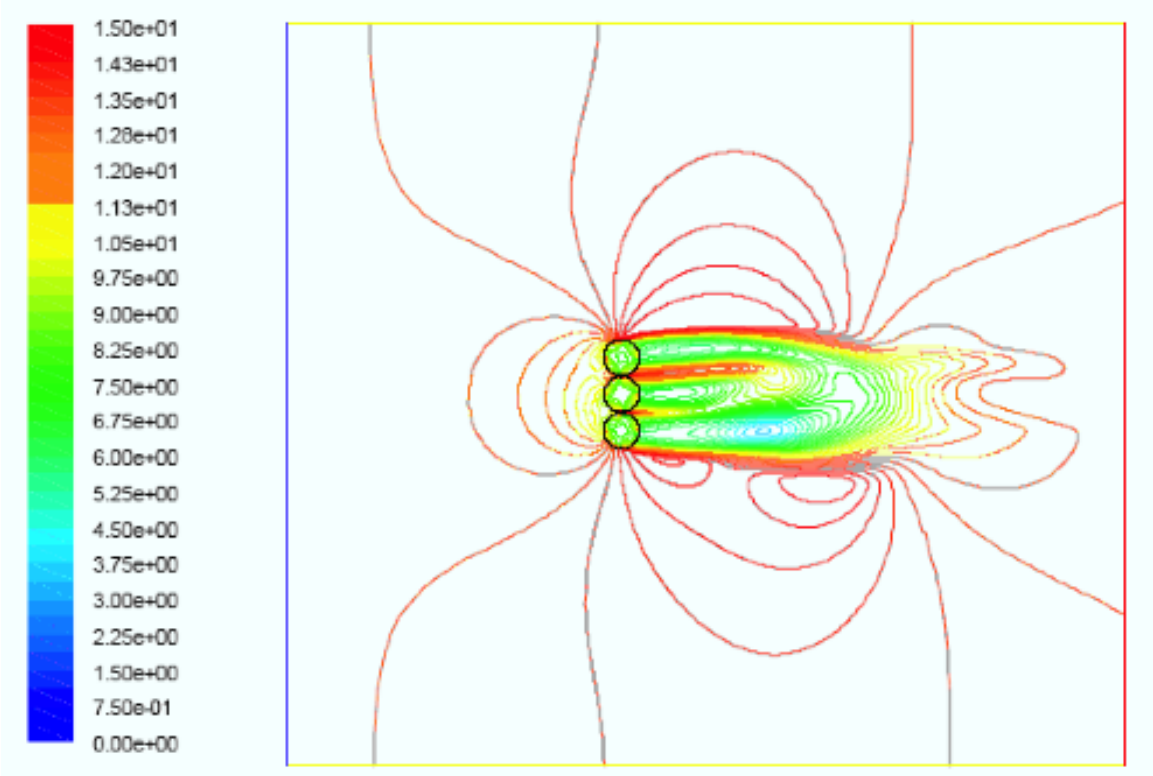

Figure 9: Average X velocity for three WHI 530G rotors

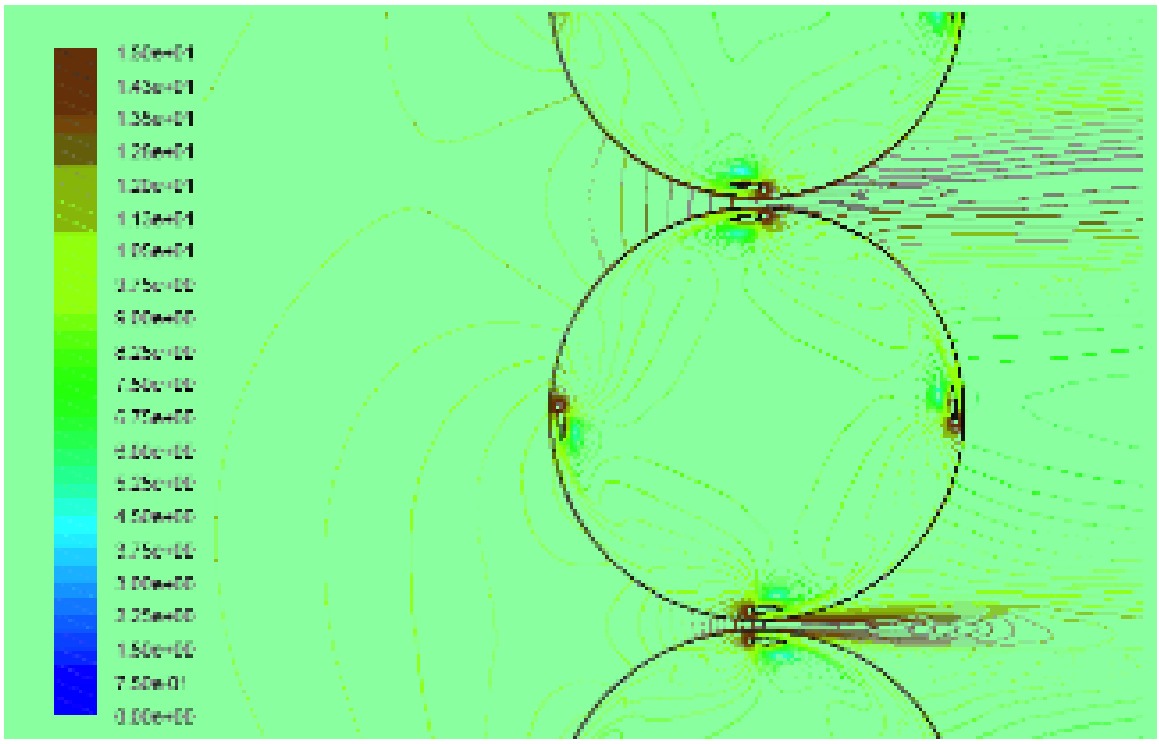

Figure 10: Close up of the average X velocity for three WHI 530G rotors

The torque on one blade is also compared for the one rotor case versus the three rotor case. Figure 14 plots the torque as a function of azimuth angle for a single blade for

TSR=2. Note that the rotation of the blades may be in opposite direction because the rotor in the middle of the three rotors array rotates clockwise. To account for this difference the azimuth angle is measured clockwise for the three rotors case. In these figures the zero azimuth angle is calculated from the direction facing the wind. From this figure we observe that the torque is increased when the blade is in the first quadrant (-90° to 0°) and in the leeward path of the rotor (120° to 210°). Figure 15 presents an amplification factor which is the difference of torques divided by the average torque of the one rotor case. This amplification factor reaches 2.5 in the first quadrant and 1.5 in the leeward path of the rotor. The surface under this curve also indicates that both increases are equally important for the overall increase in torque. The average torque ratio between the three rotors case and the one rotor is 1.27 at TSR = 2.

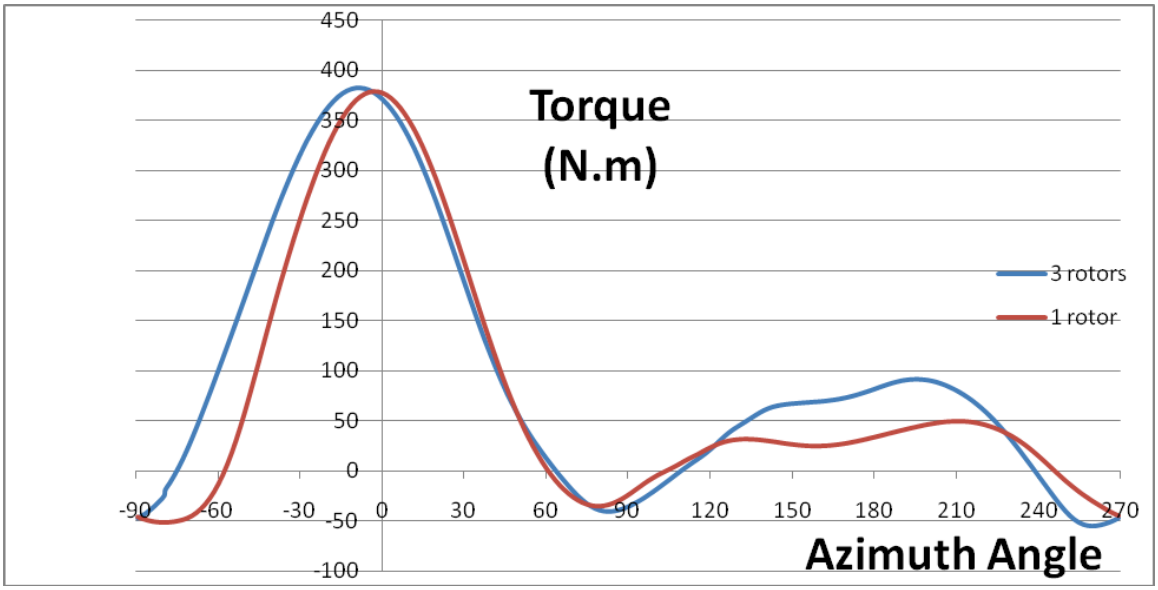

Figure 14: Comparison of torque on 1 blade for between the on1 and three rotors case

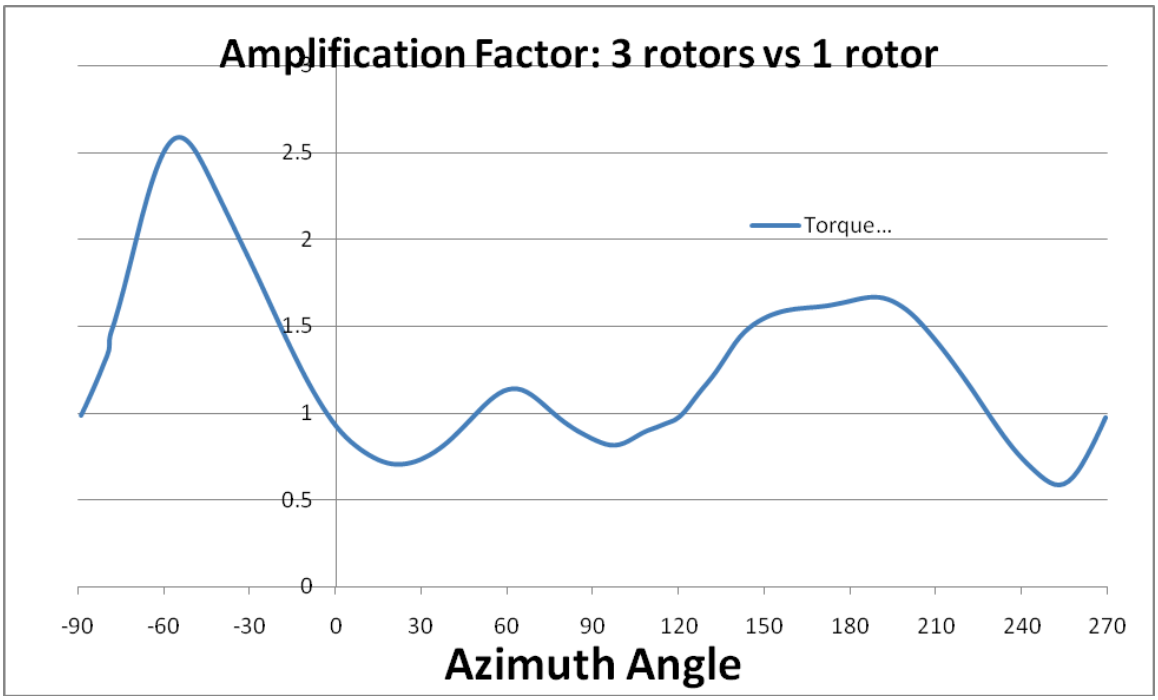

Figure 15: Amplification factor between one and three rotors

CFD model for multiple WHI 3000 turbines:

CFD is also used to simulate the flow over three WHI 3000 type rotors placed in a linear array as shown in figure 16. Similarly, the top rotor is rotating counter clockwise, the middle rotor is rotating clockwise and the bottom rotor is rotating counter clockwise. This simulation assumes a two dimensional flow as in the case of 1 rotor. The distance between the rotors axis is 1.08 rotor diameters which is a bigger gap in terms of the chord length than in the previous case.

Figure 16 and 17 are illustrations of results obtained for TSR =2 and time step of 0.0065. The flow around one blade is presented in Figure 18. In this case, there is less asymmetries of the iso-contours which indicate that the vortex effect is weaker.

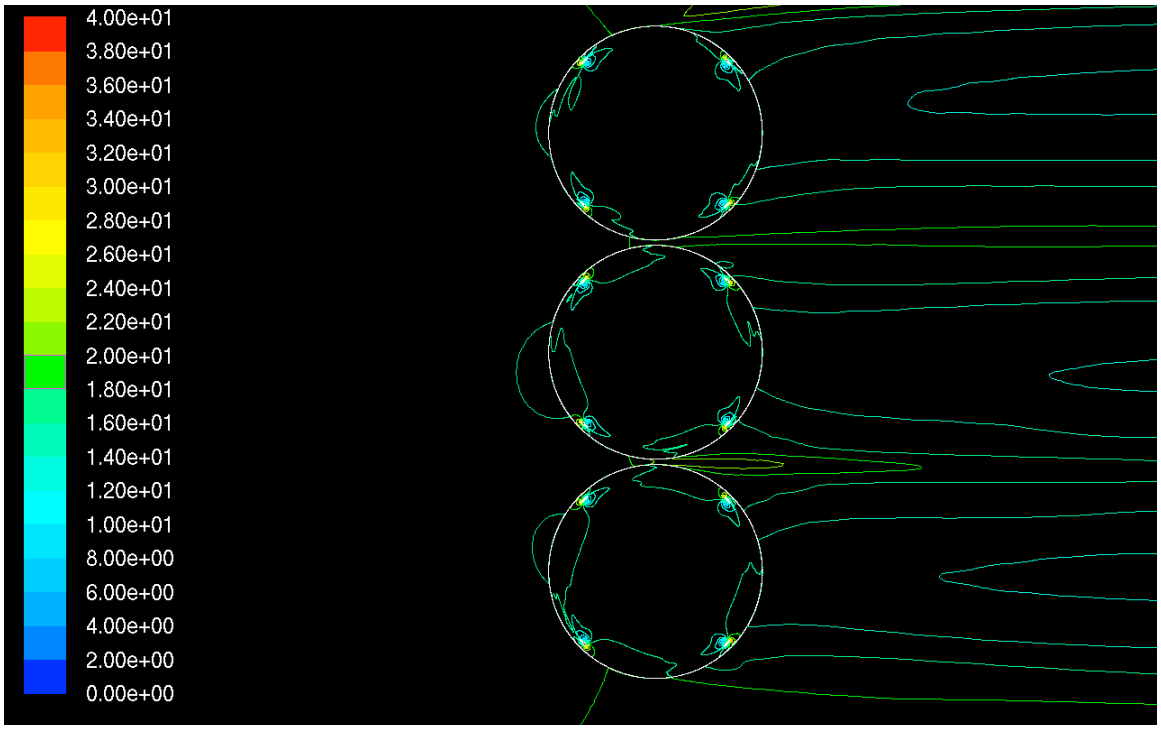

Figure 16: Time average x velocity iso-contours for an array of three WHI 3000 turbines.

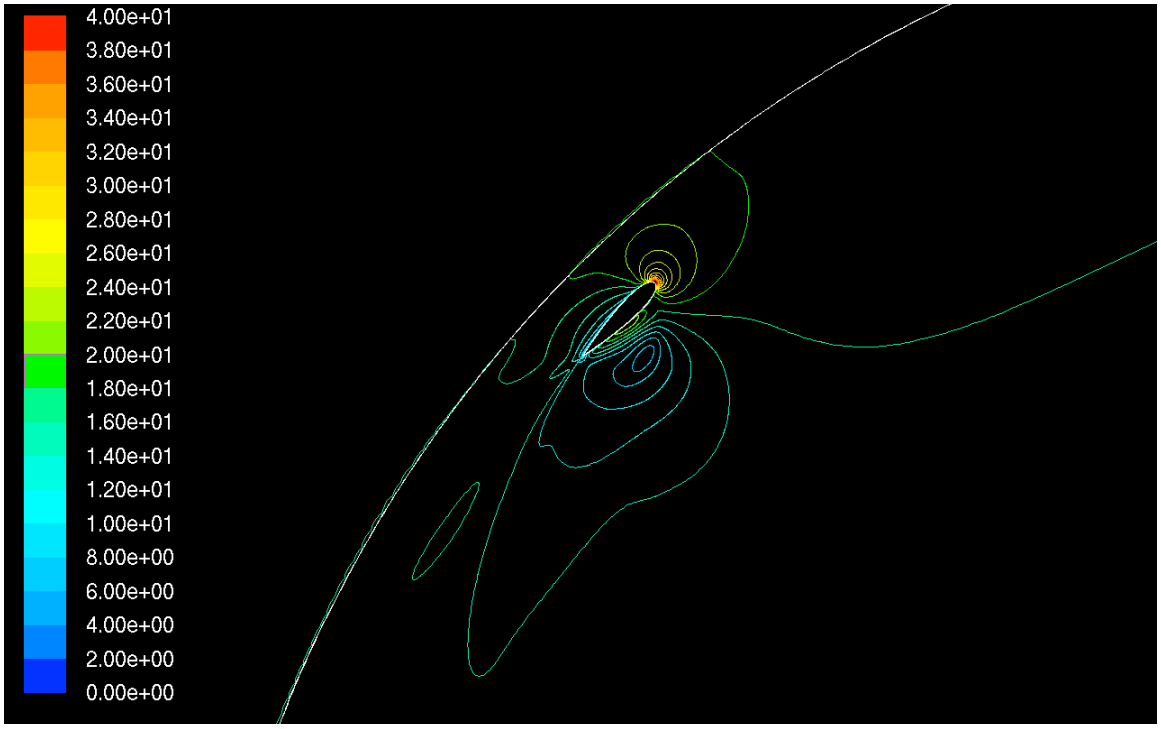

Figure 17: Velocity iso-contours around one blade for an array of three WHI 3000 turbines.

The time history of the power coefficient as a function of iteration number for the four TSR calculations are reported in Figure 18. Note that, as the TSR increases, the number of iterations needed to achieve a constant amplitude oscillatory flow is higher leading to more computational run time.

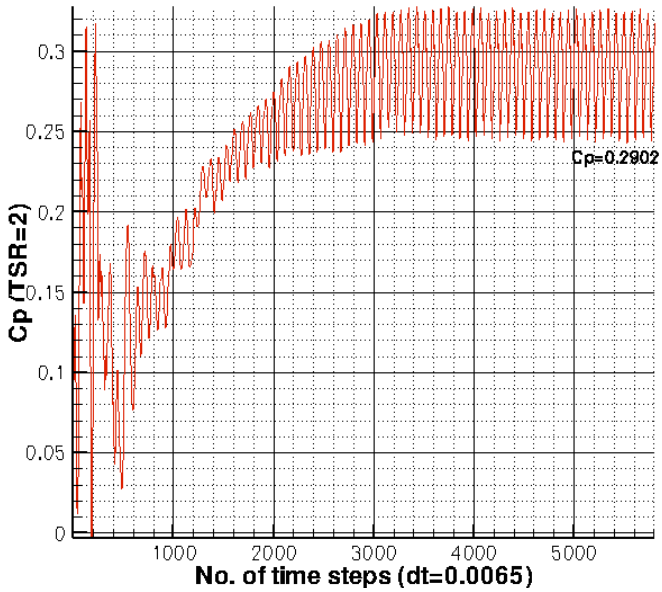

Figure 18a: Power coefficient as a function of number of iterations at TSR 2.

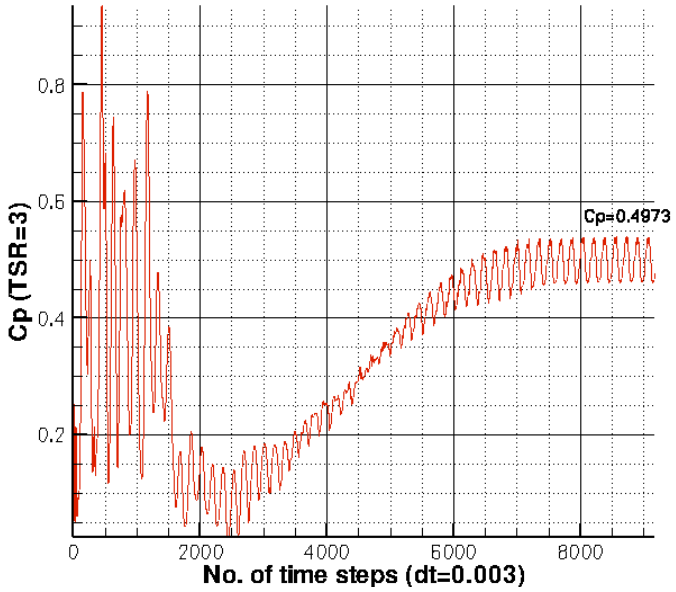

Figure 18b: Power coefficient as a function of number of iterations at TSR 3.

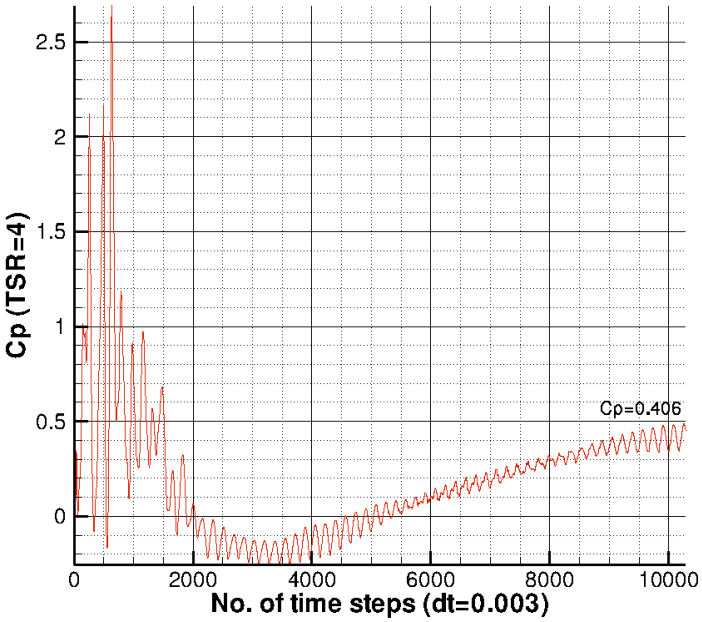

Figure 18c: Power coefficient as a function of number of iterations at TSR 4.

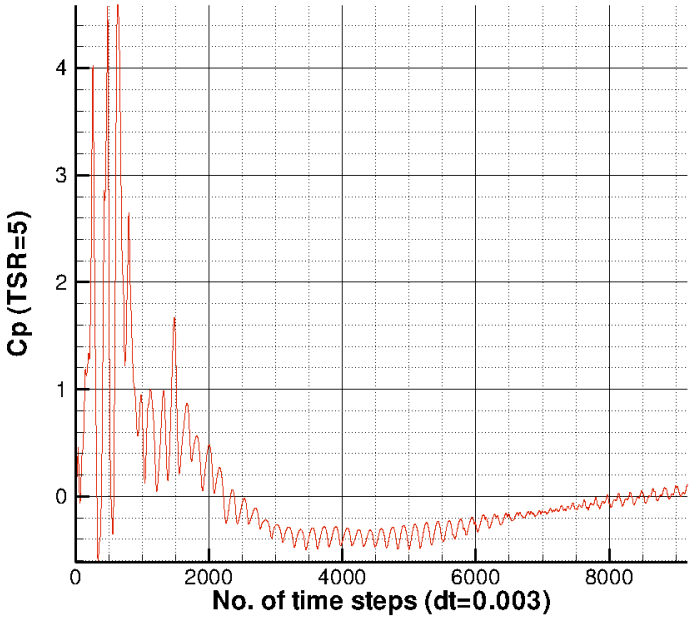

Figure 18d: Power coefficient as a function of number of iterations at TSR 5.

Table 5 reports the value of the power coefficient for one and three WHI 3000 turbines. At low TSR - high wind velocities - the increase in power coefficient reaches 23% . As seen in Figure 18d, the coefficient of power as a function of iteration number has not yet

reached a constant average value. Nevertheless we see that the value of power coefficient is small.

Table 3: Power coefficient comparison for 1 and 3 rotors based on CFD calculations.

Cp CFD results	*1 rotor*	*3 rotors*
TSR = 2.0	0.26	0.29
TSR = 3.0	0.43	0.497
TSR = 4.0	0.33	0.406
TSR = 5.0	0.153	

2. Analysis of the vortex effect

CFD of multiple WHI 530G turbines at different rotation speeds.

In this section the behavior of the middle turbine is analyzed when the top turbine is rotated at different speeds. Recall that the top turbine in an array of three turbines is rotating counter clockwise. Two different rotation speeds are used. First the top turbine is rotating at 180 RPMs which is double the speed of its nominal speed. In this case the coefficient of power of the middle turbine increased by another 19% to 0.381. Clearly the vortex effect increased the CP. Figure 19 also shows this increase. The new curve (green) shows the torque as a function of the azimuth angle. Note that the other two curves present the torque for a single rotor and an array of rotors as in Figure 14. From the figure we can clearly see the effect of the vortex. In the first quadrant the velocity is increased and the blade provides more torque. Furthermore, in the forth quadrant the velocity is also increased and the torque is also increased.

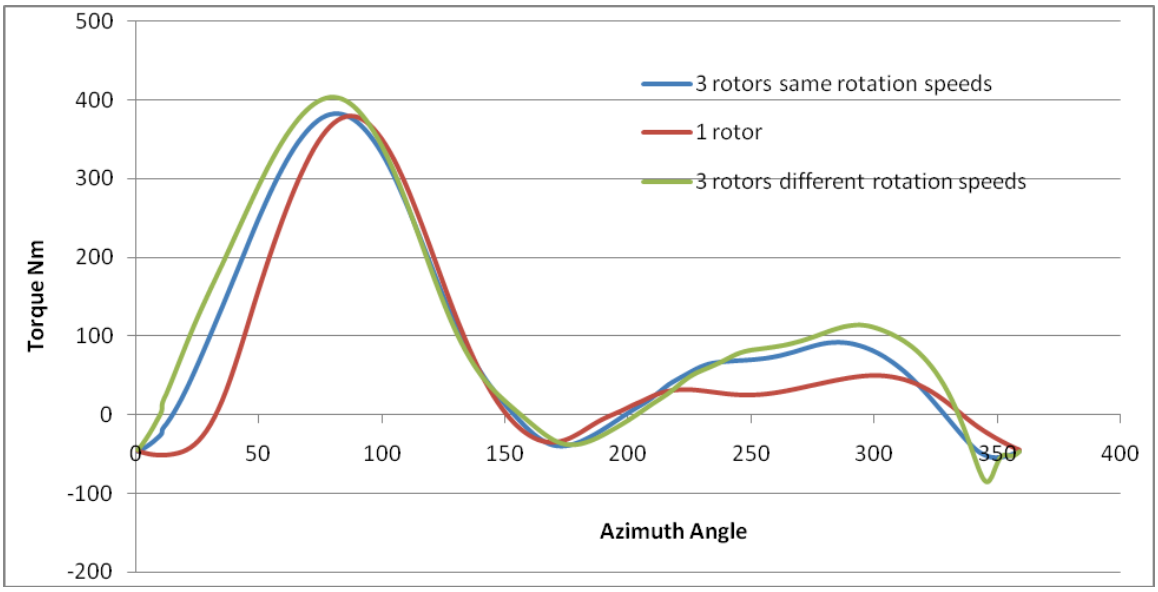

Figure 19: comparison of torque for an array of three turbines with different rotation speeds.

Additionaly, the top turbine's rotation speed was half of its nominal speed at 45 RPMs. In this case the coefficent of power obtained was 0.329 which is close to the nominal case when all three rotors rotate at the same speed. It is observed that even when the vortex effect is decreased the blockage effect remains which accounts for a respectable increase in the coefficent of power.

Analysis of stream-tube blockage effect

Figure 6 shows a single rotor and Figure 10 shows the middle rotor from an array of three rotors. The iso-curves are the x velocity and the color shows the magnitude. The same legend is used in both figures. The average wind is 12.65 m/s and is represented by orange iso-contours. For the single rotor, we note that the flow is accelerated around the rotor. The red color isocurves and the fact that they are very close together illustrate this acceleration. This is due to the fact that the turbine acts as an obstruction forcing a portion of flow to go around it. Obviously the flow also flows through the rotor and this is related to solidity of the turbine. Similarly for an array of rotor the flow wants to accelerate around it but the adjacent rotor is so close that the flow has to accelerate both in the gap between the two rotor and through the rotor. Note that the there are yellow iso-curves in the wake of the rotor where there were only green iso-curves in the case of one rotor. In conclusion, due to the fact that the flow is confided by the proximity of another rotor the wind speed increases not only between the blade of two adjacent rotors but also through the rotor. Note that a portion of the increase in torque is due to the increase in wind speed through the rotor, i.e. when the blade is travelling in the downwind part.

Analysis vortex effect at low rotation speeds The vortex effect on the WHI 3000 is analysed. The torque on a single blade for one rotor and three rotors is compared. The case investigated is for a TSR = 3 and a fixed rotation speed of 29 RPM. Based on CFD calculations, the coefficient of power is equal to 0.43 for a single rotor and 0.497 for the array of three rotors. Figure 2 compares the torque as a function of the azimuth angle. The first 180° represent the region when the blade is in the upwind part of the rotor while the second part represents the region when the blade is in the downwind part of the rotor. We see that the increase in torque happens when the blade is crossing the downwind part of the rotor. Note that we do not see any increase in the upwind region. The vortex effect must be very small as the rotation speed is low.

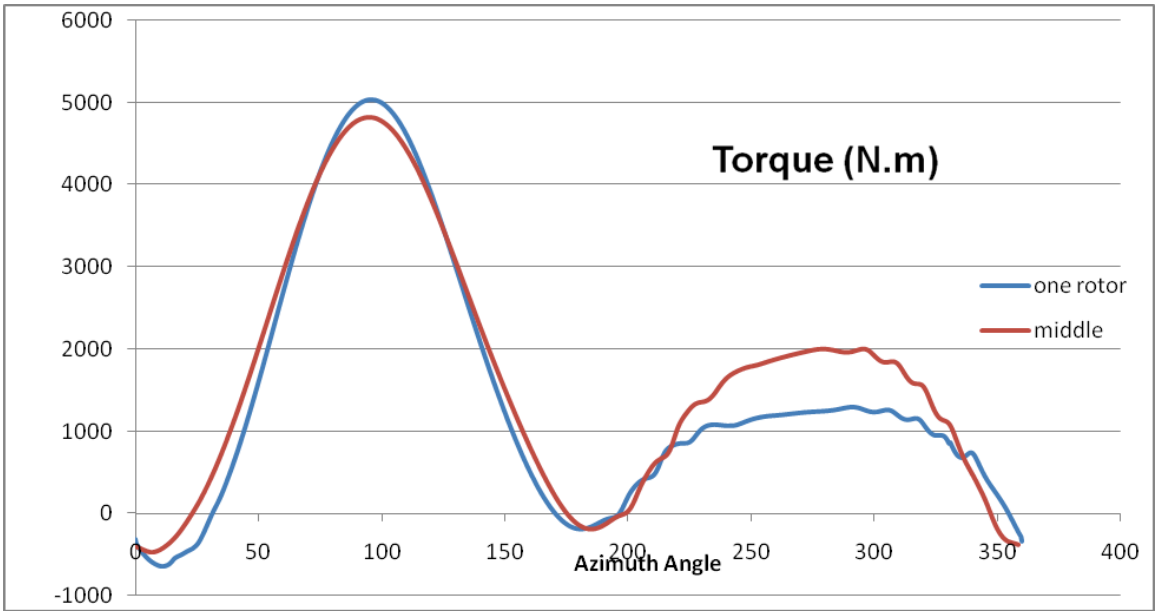

Figure 20: Comparison of torque on 1 blade for a single rotor and an array of three rotors.

We now compare the torque on one blade for the top and the bottom rotors to the middle rotor. The coefficient of power of the top rotor is 0.4975 and 0.5062 for the bottom rotor. First in the upwind region the curve representing the torque for the blades of both the top and the bottom rotors are offset when compared to the torque curve of the single or the middle rotors. The top rotor curve (blue line) is moved to the right which indicates a higher torque when the blade is in close proximity of the blade in the middle rotor. Similarly, the torque curve of the bottom rotor blade is offset to the left which indicates that the bottom rotor blade has a higher torque when it is closer to the middle rotor blade, i.e. in the first quadrant. The overall effect of this offset in negligible on the total torque as the overall area under the curves seems to be unchanged.

Second, in the downwind region, all the rotors in the array have a higher torque than the single rotor. This region accounts for the increase in the total torque and the increase in the coefficient of power.

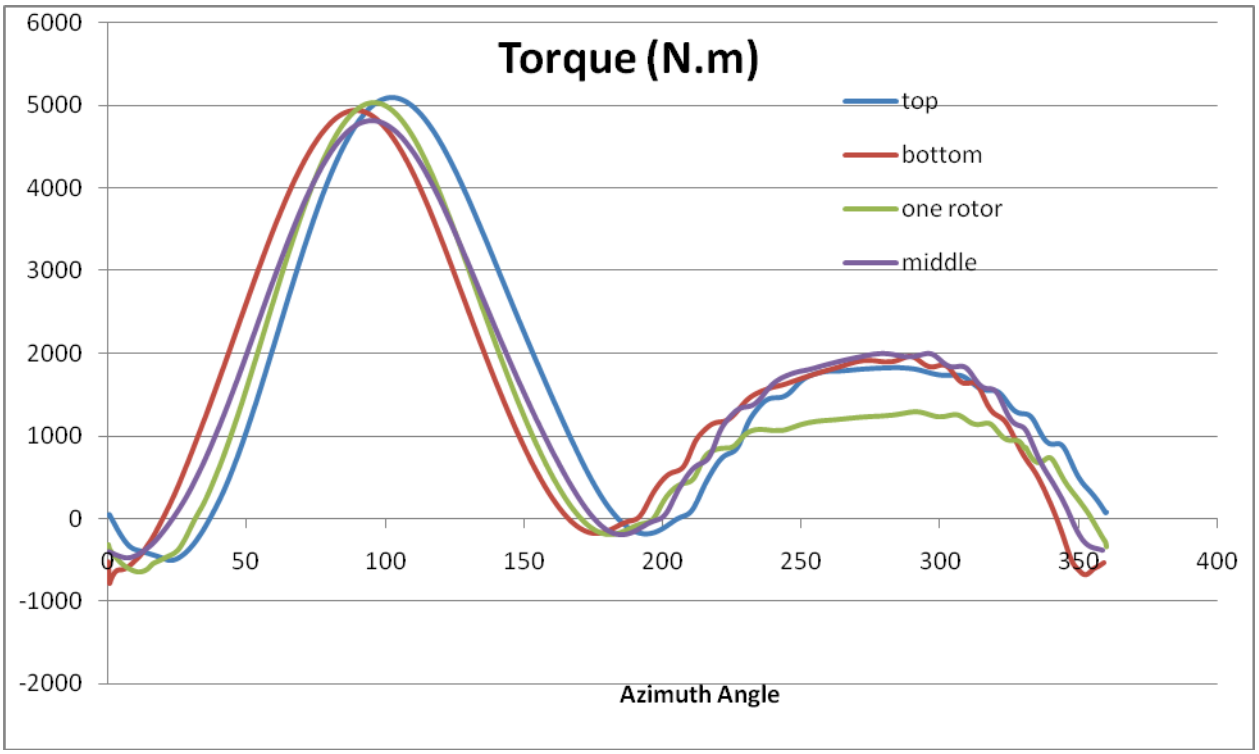

Figure 21: Comparison of torque on 1 blade for the top rotor, the bottom rotor, the middle rotor and the single rotor.

Conclusions:

In this work it is shown that CFD can accurately predict the coefficient of power, nevertheless it did require significant calibration because the turbulence models are not well adapted for highly separated boundary layer flows. Note also that the CFD is very sensitive to the mesh characteristics and require long computational time. Each TSR run takes about three days on an eight processor computer.

The comparison between one rotor and three rotors clearly demonstrates that the proximity of the rotors increases the power coefficient. The analysis also shows that the torque on each blade is increased in the first quadrant when the neighboring turbine is rotating at high rotation speed so that it induces an additional velocity field. The blades also see an increase in the torque for the leeward of the cycle. This increase can be attributed to the blockage effect.

All three rotors have a higher torque in an array configuration when compared to a single rotor. The coefficient of power is increased by 15.5% for all three rotors in the case of the WHI 3000. For low rotation speeds the increase happens when the blade travels in the leeward path of the rotor. In the upstream region the torque curve is offset for both the top and bottom rotors but the net effect is negligible.

We believe that CFD analysis can also be used to identify the best placement of VAWTs. Parameters such as distance between rotors and linear array versus a staggered

configuration should be analyzed. The effect of the wind vector for the linear array of rotors should be simulated to verify that the coefficient of power is not decreased significantly for large wind angles.

References

1. M.R. Patel. *Wind and Power Solar Systems*, CRC Press, Boca Raton (1999).

2. R.C. Bansal, T.S. Shatti and D.P. Kothari, "On some of the design aspects of wind energy conversion systems". *Energy Convers Manag* **43** 16 (2002), pp. 2175–2187

3. I. Ammara, C. Leclerc and C. Masson, "A viscous three-dimensional differential/actuator-disk method for the aerodynamic analysis of wind farms." *J Sol Energy Eng* **124** 4 (2002), pp. 345–356

4. R.J. Barthelmie, S.C. Pryor, S.T. Frandsen , et al., "Quantifying the Impact of Wind Turbine Wakes on Power Output at Offshore Wind Farms", ***JOURNAL OF ATMOSPHERIC AND OCEANIC TECHNOLOGY*** **27 8** (2010) pp: **1302-1317**
5. M.R. Soltani, M. Mahmoudi, "Measurements of velocity field in the wake of an oscillating wind turbine blade" ***AERONAUTICAL JOURNAL*** , **114 1158** (2010) pp. **493-504**

6. T. Zheng, S.K. Tang, B. Fei, "On the Forces and Strouhal Number in the low Reynolds Number Wakes of two Cylinders in Tandem", *Transactions of the Canadian Society for Mechanical Engineering*, 33 3 (2009), pp. 349-360

7. R.N. Thomas, "Coupled vortex vertical axis wind turbine", Patent # 6784566, United States Patent, 2004

8. Sandra Eriksson, Hans Bernhoff, Mats Leijon, "Evaluation of different turbine concepts for wind power", *Renewable and Sustainable Energy Reviews*, Volume 12, Issue 5, June 2008, Pages 1419-1434

9. Paraschivoiu, *Wind Turbine Design With Emphasis on Darrieus Concept*, Presse Internationales Polytechniques, 2002.

10. R.W. Whittlesey, S. Liska, J.O. Dabiri "Fish schooling as a basis for vertical axis wind turbine farm design" ***BIOINSPIRATION & BIOMIMETICS*** **5 3** (2010) Article Number: **035005** Published: **SEP 2010**

11. J. Sumner, C.S. Watters, C. Masson, "CFD in Wind Energy: The Virtual, Multiscale Wind Tunnel" *Energies* Volume: 3 Issue: 5 Pages: 989-1013 Published: May 2010